Glioblastoma-derived extracellular vesicles modify the phenotype of monocytic cells

Jeroen de Vrij[1], S.L. Niek Maas[1], Kitty M.C. Kwappenberg[2], Rosalie Schnoor[1], Anne Kleijn[3], Lennard Dekker[4], Theo M. Luider[4], Lot D. de Witte[5,6], Manja Litjens[5], Miriam E. van Strien[5], Elly M. Hol[5,7,8], Jerome Kroonen[1], Pierre A. Robe[1], Martine L. Lamfers[3], Marco W. Schilham[2] and Marike L.D. Broekman[1]

[1] Department of Neurosurgery, Brain Center Rudolf Magnus Institute of Neurosciences, University Medical Center, Utrecht, The Netherlands
[2] Department of Pediatrics, Leiden University Medical Center, The Netherlands
[3] Department of Neurosurgery, Brain Tumor Center, Erasmus Medical Center, Rotterdam, The Netherlands
[4] Department of Neurology, Brain Tumor Center, Erasmus Medical Center, Rotterdam, The Netherlands
[5] Department of Translational Neuroscience, Brain Center Rudolf Magnus Institute of Neurosciences, University Medical Center, Utrecht, The Netherlands
[6] Department of Psychiatry, University Medical Center, Utrecht, The Netherlands
[7] Netherlands Institute for Neuroscience, an Institute of the Royal Netherlands Academy of Arts and Sciences, Amsterdam, The Netherlands
[8] Swammerdam Institute for Life Sciences, Center for Neuroscience, University of Amsterdam, The Netherlands

Glioblastoma multiforme (GBM) is the most common primary brain tumor and is without exception lethal. GBMs modify the immune system, which contributes to the aggressive nature of the disease. Particularly, cells of the monocytic lineage, including monocytes, macrophages and microglia, are affected. We investigated the influence of GBM-derived extracellular vesicles (EVs) on the phenotype of monocytic cells. Proteomic profiling showed GBM EVs to be enriched with proteins functioning in extracellular matrix interaction and leukocyte migration. GBM EVs appeared to skew the differentiation of peripheral blood-derived monocytes to alternatively activated/M2-type macrophages. This was observed for EVs from an established cell line, as well as for EVs from primary cultures of GBM stem-like cells (GSCs). Unlike EVs of non-GBM origin, GBM EVs induced modified expression of cell surface proteins, modified cytokine secretion (e.g., an increase in vascular endothelial growth factor and IL-6) and increased phagocytic capacity of the macrophages. Most pronounced effects were observed upon incubation with EVs from mesenchymal GSCs. GSC EVs also affected primary human microglia, resulting in increased expression of Membrane type 1-matrix metalloproteinase, a marker for GBM microglia and functioning as tumor-supportive factor. In conclusion, GBM-derived EVs can modify cells of the monocytic lineage, which acquire characteristics that resemble the tumor-supportive phenotypes observed in patients.

Tumor Immunology

Despite extensive treatment, the prognosis of patients with glioblastoma multiforme (GBM), the most common primary brain tumor in adults, remains dismal with a median survival of only 15 months.[1] Many factors contribute to the malignant potential of GBMs, including the capacity of GBMs to modulate the immune system.[2] Immune modulation occurs at a systemic level, as well as in the tumor microenvironment,

and involves different types of immune cells. Most patients with GBM exhibit changes in the lymphocyte compartment, with an overall decrease in the number of CD4+ helper T-cells and a relative increase in regulatory T-cells with immune-suppressive characteristics.[3] In addition, GBMs strongly influence cells of the monocytic lineage (monocytes, macrophages and microglia).[4] The blood of GBM patients contains monocytes with altered characteristics, such as a reduced expression of receptors involved in antigen presentation.[3,5,6] Locally, GBMs are characterized by the presence of large numbers of tumor-associated macrophages (TAMs), which constitute brain resident microglia as well as macrophages derived from peripheral monocytes.[4,7,8] Although TAMs consist of different macrophages/microglia subtypes, major part of the TAM population acquires an "alternatively activated" (M2-type) phenotype.[4,7,8] As compared to the "classically activated" (M1-type) macrophages, these cells have a weakened capacity to activate the immune system, and an increased capacity to induce tissue remodeling (by stimulating vascularization and/or degradation of extracellular matrix components), and are therefore considered as tumor supportive. The accumulation and activity of the M2-type

What's new?

The prognosis of patients with glioblastoma multiforme (GBM) remains dismal. GBM tumors can modify the immune response, both locally and systemically, which contributes to the aggressive nature of the disease. In this study, the authors found that GBM-derived extracellular vesicles (EVs) were able to modify the phenotypes of immune cells such as microglia and blood-derived monocytes in ways that made them more tumor-supportive. Changes included altered cytokine secretion by macrophages and increased expression of Membrane type 1-matrix metalloproteinase (MT1-MMP) by microglia. These results suggest that blocking GBM-derived EVs may have therapeutic potential.

TAMs clearly distinguishes GBMs from lower grade gliomas.[9] GBM's ability to modify different components of the immune system may not only contribute to the tumor's aggressive proliferation and migration, but may also result in reduced efficacy of (experimental) treatments ("immunotherapies").[10] Still, the mechanisms responsible for the immune modulatory effects remain unknown.

Recently, it has been shown that extracellular vesicles (EVs), including exosomes (50–150 nm vesicles formed by fusion of multivesicular bodies with the cell membrane), mediate local and systemic cell communication.[11,12] Tumor cells were found to transfer their contents, including RNAs and proteins to different types of recipient cells, using EVs as vehicles.[13] This transfer provides a variety of tumor-supportive features to the tumor environment, for instance leading to the establishment of premetastatic niches.[14,15] EVs from GBM cells were reported to modify recipient cells (of tumor or endothelial origin) *via* the transfer of cell-transforming proteins and messenger RNAs [*e.g.*, epidermal growth factor receptor variant 3 (EGFRvIII)] and specific types of small noncoding RNAs.[16–20]

In this report, we describe the effects of GBM-derived EVs on the phenotype of monocytic cells, including peripheral-derived monocytes/macrophages and brain-resident microglia. These data identify EVs as a mechanism for GBM to modify the phenotype of monocytic cells, providing them M2-type/alternatively activated phenotypes.

Material and Methods
Cell culture
The established cell lines U87-MG/EGFRvIII (GBM) and HOG (oligodendroglioma)[21] were cultured in Dulbecco's modified Eagle's medium (Invitrogen, Carlsbad, CA) containing 10% fetal bovine serum (FBS; Invitrogen). The authenticity of the cell lines was confirmed by short tandem repeat (STR) analysis, using the AmpFLSTR®Identifiler® PCR Amplification Kit (Applied Biosystems, Foster City, CA). Mesenchymal stem cells (MSCs) were isolated from human bone marrow as described previously,[22] according to the official guidelines of the Leiden University Medical Center (LUMC, Leiden, The Netherlands). MSCs were cultured in alpha-MEM medium (Invitrogen) containing 10% FBS (Invitrogen), 2 μM ascorbic acid and 1 ng ml^{-1} bFGF. The FBS was centrifuged at 100,000g for 16 hr to remove contaminating E*V*s. Primary brain tumor cultures were established by enzymatic and mechanical dissociation from fresh tumor material collected during brain tumor surgery (Department of Neurosurgery, Erasmus Medical Center, Rotterdam; Department of Neurosurgery, St. Elisabeth Hospital, Tilburg, The Netherlands), according to a previously described protocol and approved by an institutional review board.[23,24] Tumors were classified as GBM by histological diagnosis. RNA was isolated from tumor material, followed by molecular subclassification, using previously described protocols.[23,25] Partek Software (St. Louis, MO) was used to perform Gene Set Enrichment Analysis. The tumor-derived cultures were grown as glioma stem cell-like (GSC) cultures in serum-free medium.[23] All cell cultures were maintained at 37 °C in a humidified atmosphere of 5% CO_2. Cell growth medium was supplemented with penicillin (100 units ml^{-1}) and streptomycin (100 μg ml^{-1}; Invitrogen).

Peripheral blood mononuclear cells (PBMCs) were isolated from blood after informed consent. PBMCs were obtained by Ficoll-Paque PLUS (GE Healthcare Life Sciences, Freiburg, Germany)-density gradient centrifugation. CD14+ monocytes were isolated magnetically on an LS MACS® column (Miltenyi Biotec, Bergisch Gladbach, Germany). PBMCs and monocytes were cultured in RPMI medium (PAA Laboratories GmbH, Pasching, Austria) containing 10% FBS (Invitrogen).

Isolation of EVs
EVs were isolated from cell culture supernatants and blood (Ficoll supernatants after PBMC-isolation), using previously described protocols.[26,27] Iodixanol-based density-gradient isolation (ultracentrifugation at 192,000g for 4 hr), followed by purification on a 30% sucrose cushion (ultracentrifugation at 100,000g for 40 min) was used for the side-by-side isolation of U87-MG/EGFRvIII and GS184 E*V*s.[27] Sequential ultracentrifugation (two times at 100,000g for 70 min) was used for the large-panel isolation of GBM and non-GBM E*V*s.[26] Prior to these ultracentrifugation procedures, cell culture supernatants and Ficoll supernatants were cleared from cellular debris by centrifugation (300g for 10 min, followed by 4,000g for 1 hr) and filtering (0.22-μm vacuum filter; Corning, NY).

Quantification and size profiling of EVs
Concentration and size of EVs were measured by tunable resistive pulse sensing (tRPS), using the qNano platform (Izon Science, Christchurch, New Zealand). This method relies on the detection of nanosized particles upon their movement through

Tumor Immunology

a nanosized pore and allows for reliable and rapid measurement of EVs in small sample volumes.[27] In brief, purified EVs or cell culture supernatants were spiked with polystyrene beads of known concentration and size. The samples were applied to the qNano and particle flow rates and the particle blockage magnitudes were measured. These parameters allowed for calculation of EV concentration and volume, respectively, using our previously described methods.[27,28]

Monocyte and macrophage analyses

To assess effects of EVs on nondifferentiated monocytes, PBMCs (150,000 cells) or isolated monocytes (50,000 cells) were added to a well of a 96-well round-bottom plate in 100 µl medium. EVs were isolated from cell culture supernatant (U87-MG/EGFRvIII and GS184) and from blood (healthy donors and GBM patients) and added to the cells (2×10^8 cell culture EVs per well and 10^6 blood EVs per well). After incubation for 3 days, cells were prepared for flow cytometry analysis.

Monocyte-to-macrophage differentiation was induced by culturing of monocytes (10^6 cells) with granulocyte macrophage colony stimulating factor (GM-CSF; 800 units ml^{-1}; Peprotech, NJ) in 24-well plates. EVs were added with equal amounts (0.35×10^8 EVs, as determined by tRPS) at Day 0 and Day 3 after plating. As an alternative differentiation condition, monocytes were exposed to Macrophage Colony Stimulating Factor (M-CSF; 20 ng ml^{-1}; Peprotech). After incubation for 6 days, cells were prepared for flow cytometry analysis. Cells were washed twice with PBS/0.02% sodium azide, fixed for 10 min in 4% paraformaldehyde, washed twice with PBS/0.5% BSA/0.02 sodium azide and stained with antibodies. Antibodies used were anti-CD1a (APC, clone HI149), anti-CD3 (PerCP Cy^{TM}5.5, SK7), anti-CD14 (APC, clone MφP9), anti-CD14 (FITC, clone MφP9), anti-CD14 (PerCP Cy^{TM}5.5, clone M5E2), anti-CD25 (FITC, 2A3), anti-CD32 [APC, clone FLI8.26 (2003)], anti-CD40 (FITC, clone 5C3), anti-CD45 (PerCP Cy^{TM}5.5, clone 2D1), anti-CD86 [FITC, clone 2331 (FUN-1)], anti-CD86 [PE, clone 2331 (FUN-1)], anti-CD163 (PE, clone GHI/61), anti-HLA DR (FITC, clone G46-6), anti-HLA DR (PE, L243; BD Biosciences, NJ), anti-CD33 (APC, clone D3HL60.251), anti-CD64 (FITC, clone 22), anti-CD127 (PE, R34.34; Beckman Coulter Company, Marseille, France), anti-CD3 (APC, clone UCHT1), anti-CD19 (APC, J4.119) and anti-CD56 (APC, NKH1; Immunotech). To analyze phagocytic capacity, macrophages were exposed to FITC-dextran beads (1 mg ml^{-1} for 30 min; Sigma Aldrich, FD40S, molecular weight 40,000) followed by flow cytometric quantification of FITC uptake. Flow cytometry was carried out on a FACS Calibur (Becton Dickinson) and data were analyzed using CellQuest software (Becton Dickinson). Expression levels are displayed as geometric means.

Cytokines and chemokines in macrophage supernatants were quantified with a magnetic bead-based multiplex assay (Bio-Plex Pro^{TM} Assay, Bio-Rad Laboratories, CA).

Quantitative polymerase chain reaction (qPCR) was used to quantify expression levels of Toll-like receptor 2 (TLR-2) and Membrane type 1-matrix metalloproteinase (MT1-MMP) RNA in macrophages. RNA was isolated from macrophages using the RNeasy Plus Micro kit (Qiagen, Hilden, Germany). Complementary DNA was synthesized using the SuperScript III First-Strand Synthesis System (Invitrogen) using oligo(dT) primers according to the manufacturer's protocol. SYBR Green-based qPCR (Applied Biosystems) was performed using oligonucleotides TLR-2_forward (5′-CTTTCAACTGG TAGTTGTGG-3′), TLR-2_reverse (5′-GGAATGGAGTTTAA AGATCCTG-3′), MT1-MMP_forward (5′-ATGGCAAATTC GTCTTCTTC-3′) and MT1-MMP_reverse (5′-CGTTGAAAC GGTAGTACTTG-3′). The expression levels were normalized to the expression level of Actin-β (Act_forward: 5′-GACGAC ATGGAGAAAATCTG-3′, Act_reverse: 5′-ATGATCTGGGT CATCTTCTC-3′). PCR amplification (10 min at 95 °C, 45 cycles of 95 °C for 15 sec followed by 60 sec at 60 °C, 15 s at 95 °C) was followed by melt-curve analysis. PCR amplification was performed in triplicate and for each triplicate delta CT values ($CT_{TLR-2} - CT_{Actin-\beta}$ and $CT_{MMP14} - CT_{Actin-\beta}$) were calculated.

Mass spectrometry

Highly sensitive mass spectrometry (MS) analysis was performed to quantify and compare the proteomic contents of GBM cells and their secreted E*V*s. EVs were isolated from the supernatants of U87-MG/EGFRvIII and GS184 monolayer cultures, and were, in parallel with cell pellets, dissolved in lysis buffer (*i.e.*, 2.5×10^8 EVs or 500 cells were dissolved in 50 µl RapiGest^{TM} surfactant (1 mg ml^{-1}; Waters Corporation, MA) in 50 mM ammoniumbicarbonate. Samples were stored at −80 °C until further use. After thawing, reduction and alkylation was performed by adding 2 µl of 0.5 M dithiothreitol to each sample, followed by incubation for 30 min at 60 °C. After cooling down to room temperature, 10 µl of 0.3 M iodoacetamide was added, followed by incubation in the dark for 30 min. Subsequently, 1.5 µl of 100 ng µl^{-1} gold trade trypsin (Promega, Madison, WI) in 3 mM Tris-HCL (diluted 1:10 in 50 mM NH$_4$HCO$_3$) was added to each sample, followed by overnight incubation at 37 °C. To inactivate trypsin, 3 µl of 25% trifluor-acidic acid was added and samples were incubated for 30 min at 37 °C. Next, the samples were centrifuged at 10,000*g* for 15 min at 4 °C and the supernatant was transferred to LC/MS-certified vials (Waters Corporation). For each sample, a fraction (10%) of the total volume was measured on a nanoliquid chromatography (nano-LC) system (Ultimate 3000 Nano-LC system, Dionex, Thermo Scientific, Amsterdam, The Netherlands) to determine relative concentrations. Based on these measurements, the injection volume for each individual sample could be adjusted to allow for MS analysis of equal amounts of digested samples. MS analysis was performed as described, using a coupled nano-LC system with an Orbitrap MS platform (LTQ-Orbitrap XL, Thermo Scientific).[29]

MS spectra were extracted from raw data files and converted into Mascot generic format (MGF) files using Extract-MSN (part of XCalibur (version 2.0.7), Thermo Scientific). The data files were searched by Mascot (version 2.3; Matrix Science, London, UK) against the UniProt Swiss-Prot database selected for *Homo sapiens* (20,070 entries), using the following settings: a maximum of two miss-cleavages, oxidation as a variable modification of methionine, carbamidomethylation as a fixed modification of cysteine and trypsin selected as digestion enzyme. A peptide mass tolerance of 10 ppm and a fragment mass tolerance of 0.5 Da were allowed. Scaffold proteome analysis software (version 3.6.3; Proteome Software, Portland, OR) was used to visualize protein detections and to add Gene Ontology (GO) Terms. The data files were exported to Microsoft Office Excel 2010 (Microsoft, Redmond, WA) and quantitative analyses were performed (protein filter settings: "number of spectra ≥ 1", "protein ID probability $\geq 95\%$"). Quantitative information was obtained on the relative concentration of each protein (number of spectrum counts as percentage of total spectra), as well as on protein enrichment in EVs (*i.e.*, the difference between the protein concentration in EVs and the protein concentration in the cells). Functional connectivity between proteins was assessed using the STRING 9.1 algorithm (http://string-db.org/),[30] in which the Kyoto Encyclopedia of Genes and Genomes (KEGG; www.kegg.jp) was selected as pathway source. Connections between proteins were visualized as "confidence view," with stronger associations represented by thicker lines.

Statistical analyses

Data analysis was performed using SPSS 20.0 (SPSS Inc, Chicago, IL) or Microsoft Excel 2010 (Microsoft corp., Redmond, WA). Normality of data was tested using the Shapiro-Wilk test and visualized by Q-Q plots. Equality of variance was tested using Levene's test. Two-tailed independent *t*-tests, corrected for inequality of variance if present, were used to test differences in means. In case of non-normal distributed data the Mann–Whitney *U* test was used. MS results were tested for differences in protein levels and differences in GO annotations using Fisher's exact test. Significance was determined as $p < 0.05$ unless stated otherwise. Error bars display means $\pm$ standard error of the means (SEMs).

Results

GBM EVs are enriched with specific types of proteins

We performed a detailed characterization of the EV proteome to obtain better insight into the role of EVs as carriers of cell-transforming proteins. Besides the routinely used cell line U87-MG/EGFRvIII, the primary GBM stem cell-like culture GS184 was used as a source of EVs. GS184 represents GBM more faithfully as a result of reduced accumulation of (epi)genetic alterations upon cell culturing.[24] Both cultures were found to secrete EVs. The size-distribution profiles (ranging from approximately 90–180 nm, mode 120 nm)

were highly similar (size-profile of U87-MG/EGFRvIII as reported previously,[27] the size-profile of GS184 as Supporting Information Fig. S1). Using mass-spectrometry (MS), 215 and 125 proteins were detected for U87-MG/EGFRvIII EVs and cells, respectively. Slightly more proteins were detected for GS184 EVs and cells; 287 and 300, respectively. (Refer to Supporting Information Table S1 for a complete overview of all detected proteins.) The different architecture of cells and EVs was reflected in Venn diagrams (Fig. 1a), which demonstrated the majority of proteins to be uniquely detected in either EVs ("EV-specific") or cells ("cell-specific"). The stem cell-like phenotype of GS184 was confirmed by the abundance of the neural stem cell marker *nestin* (Supporting Information Table S1). For GS184, the most abundant EV-specific proteins were chondroitin sulfate proteoglycan 4, prostaglandin F2 receptor negative regulator and disco-interacting protein 2 homolog B. For U87-MG/EGFRvIII, the most abundant EV-specific proteins were alpha-2-macroglobulin, EGF-like repeat-discoidin I-like domain-containing protein 3, and hemoglobin subunit beta. Remarkably, GS184 EVs and U87-MG/EGFRvIII EVs shared several abundant proteins, including chondroitin sulfate proteoglycan 4, alpha-2-macroglobulin, lactadherin, EGFR and different types of integrins (Supporting Information Table S1). Gene Ontology classification revealed that both cells and EVs are abundant in proteins of *cytoplasmic-*, *intracellular organelle, organelle part* or *plasma membrane* origin (Fig. 1b). However, EVs are relatively enriched with proteins of *extracellular region*, *membrane* or *plasma membrane* origin, while proteins of *cytoskeleton*, *nuclear* or *organelle part* origin are relatively scarce (Fig. 1c). This clearly reflects the differences in architecture between cells (*e.g.*, containing a nucleus, organelles and cytoskeleton) and EVs.

We speculated that GBM cells may benefit from the selective incorporation (and thereby transfer) of certain types of proteins in EVs. A list of the EV-enriched *plasma membrane* and *cytoplasmic* proteins is provided in Supporting Information Table S2. Of interest, protein pathway analysis, which included a database of hundreds of pathways, identified a few protein pathways that were significantly enriched in the membrane of the EVs; *regulation of actin cytoskeleton-*, *ECM-receptor interaction*, *focal adhesion* and *leukocyte transendothelial migration* (Supporting Information Fig. S2). The same pathways appeared to be enriched in the U87-MG/EGFRvIII EVs as in the GS184 EVs, despite the intrinsic differences between the two cell types. The selective enrichment of proteins involved in leukocyte recruitment and focal adhesion mechanisms (which are especially functioning in monocytic leukocytes to stimulate proliferation, movement and phagocytosis[8]) triggered us to further investigate the influence of GBM derived EVs on monocytes and macrophages.

GBM EVs modify monocytes

We pursued an *ex vivo* screening approach to gain insight in the effects of GBM EVs on leukocytes (Fig. 2a). Remarkably,

Tumor Immunology
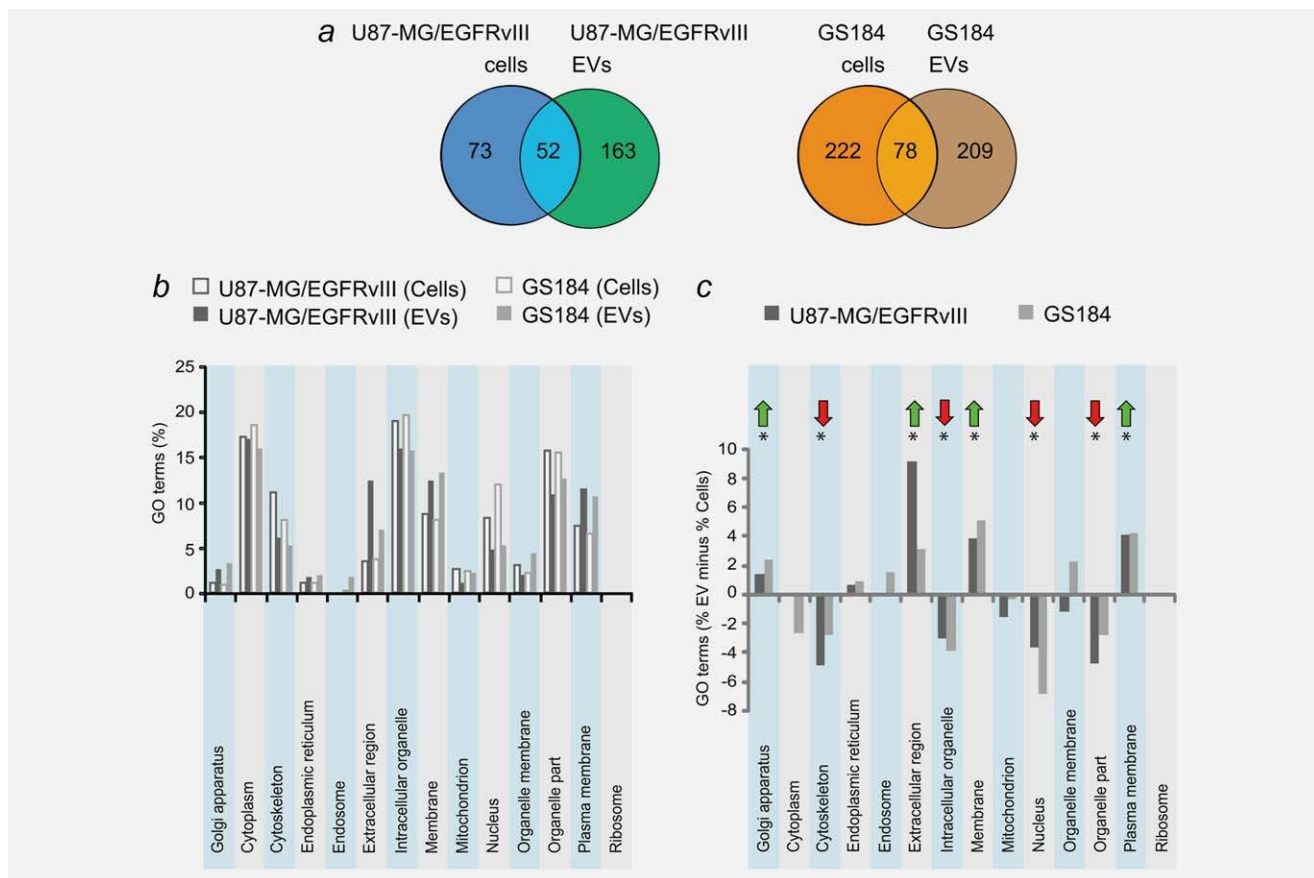
Figure 1. Proteomic analyses of U87-MG/EGFRvIII- and GS184-derived EVs. (*a*) Venn diagrams summarizing the number of proteins detected by MS analysis. Detection is grouped as "cells-only," "EV-only" or "cells and EV shared." (*b* and *c*) Assignment of *subcellular origin* GO terms to proteins. Graph (*b*) shows the relative distribution of GO terms within the proteome of either U87-MG/EGFRvIII cells, U87-MG/EGFRvIII EVs, GS184 cells or GS184 EVs. Graph (*c*) shows differences in GO term annotation between EVs and their donor cells, obtained by subtracting the cell-associated percentages from the EV-associated percentages. Significant EV-*versus*-cell differences ($p < 0.001$ for GS184 and U87-MG/EGFRvIII) are indicated with arrows. [Color figure can be viewed in the online issue, which is available at wileyonlinelibrary.com.]

incubation of PBMCs with GS184 EVs severely affected the monocytic population, demonstrating a decrease in cell surface expression level of HLA-DR (control: MFI = 730.4; EV: MFI = 223.4) and an increase in the expression of CD14 (control: MFI = 21.2; EV: MFI = 260.6; Fig. 2*b*). We obtained similar results with EVs from U87-MG/EGFRvIII cells (Supporting Information Fig. S3*d*), again showing a decrease in HLA-DR expression (control: MFI = 263.7; EV: MFI = 119.9). CD14 expression was not modified by the U87-MG/EGFRvIII EVs. In addition to these effects on cell surface markers, the GS184 EVs also affected the survival of monocytes (Fig. 2*b*). The viability of the control monocytes dramatically decreased over time, presumably caused by the absence of monocyte-survival factors, such as GM-CSF. However, in the presence of EVs this reduction was less severe (control incubation: 3.5% monocytes; EV incubation: 7.0% monocytes). The effects of the EVs on monocytes occurred in a direct manner (*i.e.*, without the involvement of other leukocyte cell types), since similar effects were observed on puri-

fied monocytes (Fig. 2*c*). In this context, the effect on monocyte survival was even more pronounced (control incubation: 5.6% monocytes; EV incubation: 44.1% monocytes). Exposure of GS184 EVs to PBMCs from another donor showed similar results (Supporting Information Figs. S3*a* and S3*b*). No effects were observed on the viability and surface marker expression (CD25) of T lymphocytes (Supporting Information Fig. S3*c*).

It has previously been shown that the blood of GBM patients contains monocytes with an aberrant phenotype, in particular characterized by a reduced cell surface presentation of HLA-DR.[6,31,32] We speculated that the EVs secreted by GBM cells may enter the systemic circulation and may subsequently modify the phenotype of monocytes. However, we did not observe an effect on the expression of cell surface markers (*i.e.*, HLA-DR and CD14) after exposing healthy monocytes with EVs from patient's blood (*i.e.*, the total pool of EVs, consisting of nontumor EVs plus a minor fraction of GBM EVs; Fig. 2*d*).
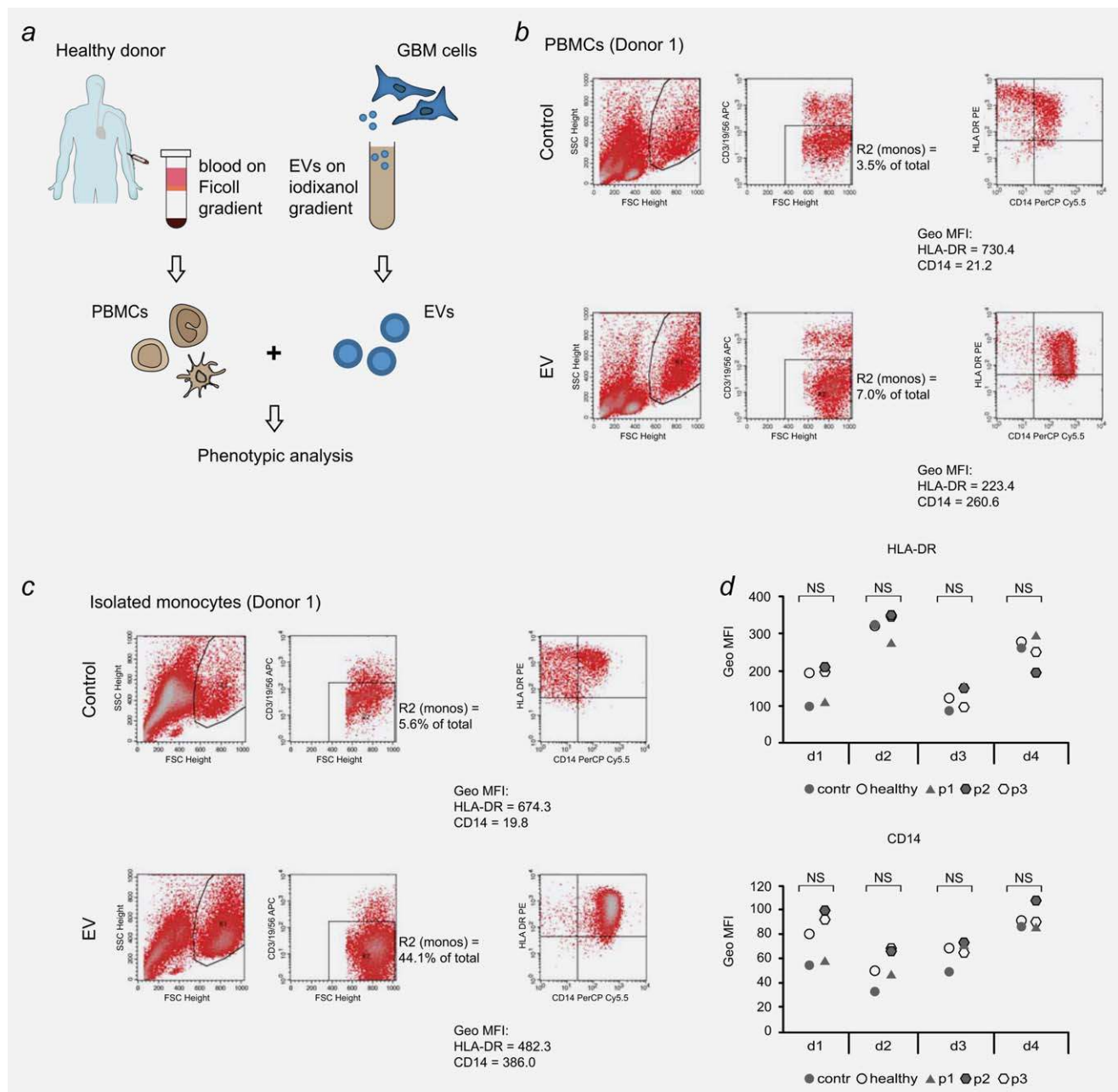
Figure 2. GBM-derived EVs modify the phenotype of monocytes. (*a*) Schematic illustration of the experimental set-up to screen for effects of GBM EVs on PBMCs. Isolation of EVs from cell culture (using iodixanol-based density gradient centrifugation) and isolation of PBMCs (using Ficoll-based density gradient centrifugation) are shown. (*b*, *c*, and *d*) Flow cytometric analysis of CD14 and HLA-DR on the surface of monocytes. (*b*) Incubation of total PBMCs (from healthy Donor 1) with GS184-derived EVs or PBS only (control). (*c*) Incubation of purified monocytes (from healthy Donor 1) with GS184-derived EVs or PBS only (control). (*d*) Incubation of PBMCs [from four healthy donors (d1–d4)] with "EV pools" (that is, all blood-residing EVs are included) from the blood of GBM patients (p1–p3), a healthy donor, or PBS only (control). The monocyte populations were defined by gating on R1 (FSC, SSC) and R2 (CD3^{neg}, CD19^{neg}, CD56^{neg}). Monocyte percentages (expressed as fraction of the total number of PBMCs) are indicated in the dotplots of (*b*) and (*c*). [Color figure can be viewed in the online issue, which is available at wileyonlinelibrary.com.]

GBM EVs affect the differentiation of monocytes to macrophages

The observed effects on monocytes prompted the question whether GBM EVs can affect the differentiation of monocytes into macrophages. As the effects of EVs may vary between different GBM cultures, we included EVs from a panel of primary GSC cultures, obtained from different patients. (Patient information is shown in Supporting Information Table S3). The cultures showed differences in growth pattern, varying from monolayers to spheres (Fig. 3*a*). Using tRPS, we were able to accurately quantify EV secretion per cell (Fig. 3*b*).
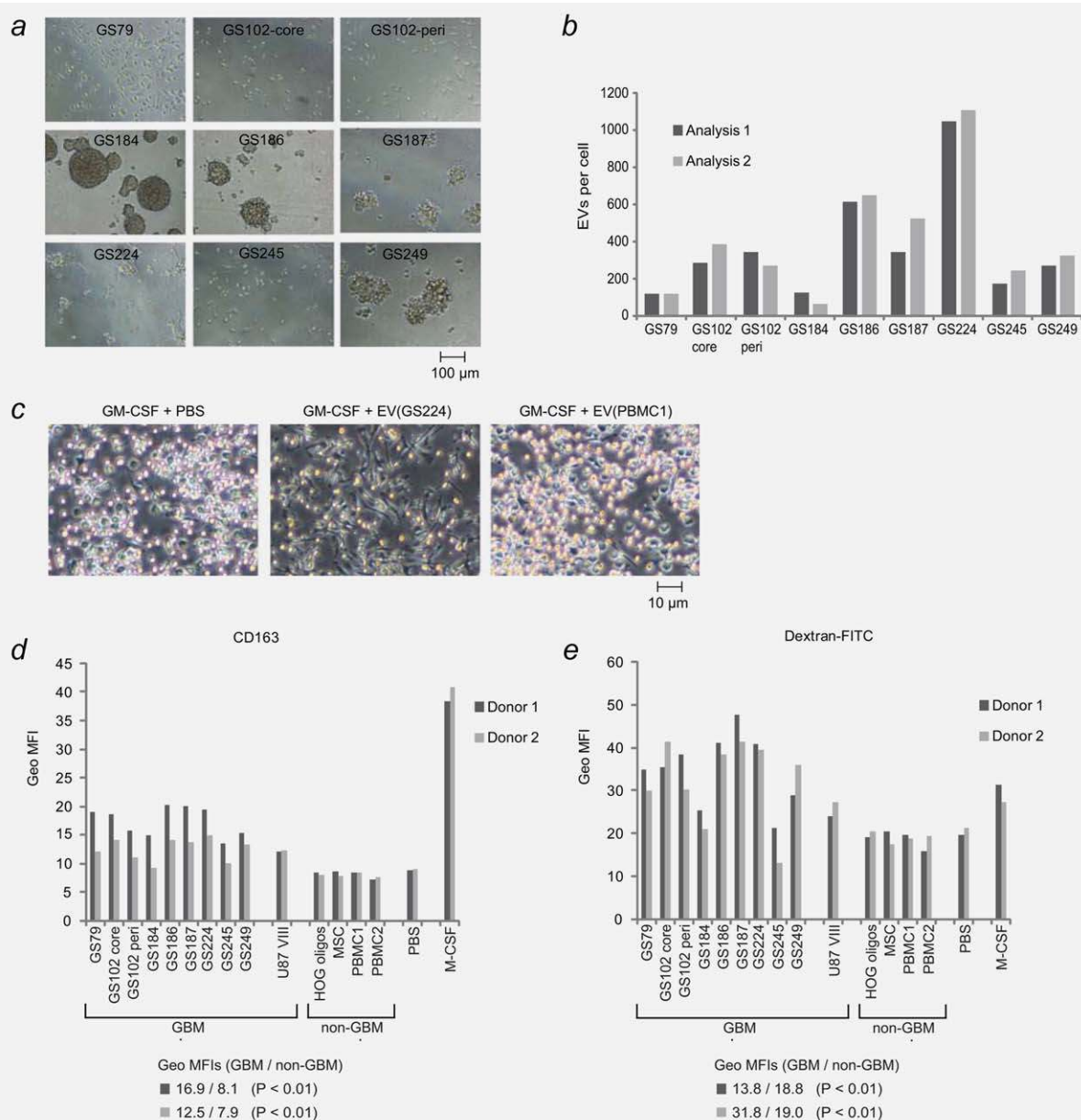
Figure 3. GBM-derived EVs modify monocyte to macrophage differentiation. (*a*) GSC cultures (grown as "neurospheres") were established from tumor material and subsequently used for EV isolation. Phase contrast microscopy showed differences in cell growth appearance. Cultures GS102-core and GS102-peri were obtained from different locations of the tumor, from, respectively, core and peripheral region. (*b*) tRPS-based quantification of GSC-derived E*V*s. EV secretion per cell (based on the number of cells at the moment of harvesting EVs) was calculated. Two independent analyses were performed. (*c*, *d*, and *e*) Addition of EVs to the culture medium upon GM-CSF-induced differentiation of monocytes to macrophages. GBM-derived EVs (from nine GSCs and U87-MG/EGFRvIII cells), as well as non-GBM-derived EVs [from HOG cells, MSCs and blood of two healthy donors (PBMC1, PBMC2)] were included. To facilitate comparison, the different types of EVs were added at equal numbers. (*c*) Representative microscopy pictures showing a differential effect of GBM EVs on the morphology of macrophages. As compared with control incubations [PBS only or EVs from blood of a healthy donor ("EV-PBMC1")], incubation with GBM EVs yielded macrophages that were relatively stretched. After incubation with non-GBM EVs, a large fraction of the cells detached and increased light scattering. (*d* and *e*) Flow cytometry-based phenotyping of macrophages. As compared to the non-GBM EV incubations, the presence of GBM EVs results in increased cell surface expression of the macrophage M2-type marker CD163 (*d*) and increased uptake of dextran-FITC beads (*e*). M-CSF incubation was included as a positive control for differentiation to M2-type macrophages. Incubations were performed with monocytes of two independent donors. For each donor, the mean values are depicted for the GBM group and the non-GBM group. Statistical significance of this difference (determined by a two-tailed *t*-test) is indicated. [Color figure can be viewed in the online issue, which is available at wileyonlinelibrary.com.]

This revealed large differences between the cultures, with EV secretion levels ranging from 85 EVs per cell (culture GS184) to 1,050 EVs per cell (culture GS224). These findings could not be attributed to the EV isolation procedure, since similar quantification results were obtained on nonpurified culture supernatants (data not shown).

The isolated EVs were added to monocytes, which were differentiated to M1-type macrophages using the cytokine GM-CSF. Besides the GSC-derived EVs, EVs were included from U87-MG/EGFRvIII cells, HOG cells (low-grade glioma), mesenchymal stem cells and blood of healthy donors. Remarkably, all GBM-derived EV preparations similarly affected the monocyte-to-macrophage differentiation, while effects were absent or less stringent for the EVs of other origin. The difference between incubation with tumor and non-tumor EVs was readily seen by standard microscopy, revealing a large proportion of macrophages with irregular shapes and increased granulation after exposure to GBM EVs (Fig. 3c). Moreover, exposure to GBM EVs induced a significantly higher expression of the macrophage M2-type marker CD163, as measured by flow cytometry (Fig. 3d). In addition, significant differences in expression levels were observed for the surface molecules HLA-DR, CD14, CD16, CD32 and CD45 (Supporting Information Fig. S4). Also, incubation with GBM EVs significantly increased the phagocytic capacity of macrophages, as compared to incubation with non-GBM EVs (Fig. 3e). The results were similar for the macrophages obtained from two independent donors. Overall, the GBM EV-induced changes resembled the changes induced after incubation with the cytokine M-CSF, which was included as a control for macrophage M2-type differentiation.

Upon incubation with GBM-derived EVs, cytokine secretion of cells showed an increase in secretion of interleukin 6 (IL-6), monocyte chemoattractant protein-1 (MCP-1) and vascular endothelial growth factor receptor (VEGF; Supporting Information Fig. S5a). To gain insight in the mechanism by which GBM EVs affect the monocytes, we analyzed the expression of MT1-MMP (Supporting Information Fig. S5b). This protein is over-expressed in glioma-associated microglia and acts as an important tumor-supportive factor.[31,33,34] Expression of MT1-MMP is induced by the binding of soluble factors to TLRs (TLR-2), but the identity of these factors remains to be identified. We speculated that the differentiation of monocytes to macrophages is accompanied by an increase in MT1-MMP, in the presence of GBM EVs. However, our RNA expression analysis did not point toward such an effect (Supporting Information Fig. S5b).

GBM EVs affect microglia

Driven by our results on macrophages we performed similar analyses on microglia, since these cells are also highly abundant in the microenvironment of GBM and play important roles in the tumor's biology. We isolated primary human microglia from postmortem brain tissues of two donors. For each donor, microglia were isolated from different brain regions (GTS, gyrus frontalis medius; GFM; gyrus temporalis superior; CC, corpus callosum; SVZ; subventricular zone). In contrast to our findings on macrophages, the GSC EVs only marginally affected expression of the cell surface marker HLA-DR (Supporting Information Figs. S6a and S6b). For Donor 1, the GFM-derived microglia showed a relative increase in HLA-DR for the GS184 EV incubation (as compared with mock), while this effect was absent for the CC-derived microglia. For Donor 2, microglia from GTS and SVZ showed a relative increase in HLA-DR for the GS184 EV incubation (as compared with mock), after 72 hr incubation. This increase in HLA-DR expression was not significant (t test, GS184 incubations ($n = 3$) *versus* mock incubations ($n = 3$) at 72 hr; $p = 0.3$) Similarly, the GBM EVs did not significantly alter the expression of CD163 (Supporting Information Figs. S6c and S6d).

As outlined above, MT1-MMP is well known for its overexpression in GBM-associated microglia. Strikingly, and in contrast to our analysis on macrophages, incubation with GBM EVs demonstrated an increase in MT1-MMP expression in the microglia of both donors (Fig. 4a). Suggestive evidence for this increase was obtained after 6 hr, while the effect was significant after 72 hr (Fig. 4b).

EVs from mesenchymal-classified tumors display the strongest effects on monocytic cells

We noticed that the GSC cultures with the highest EV secretion levels (GS186, GS187 and GS224) also showed the most pronounced modulation of the monocyte to macrophage differentiation. This was not caused by adding different numbers of EVs, since these were exactly identical for all incubations. Based on this observation, we speculated that these cultures were derived from tumor material with common characteristics that belong to a specific molecular subclass. Indeed, comparison of the tumor's RNA expression profiles revealed a set of differentially expressed genes in the EV-high-associated tumors (Fig. 5a). Also, enriched gene sets were identified; *Regulation of Defense Response* and *Interferon Gamma Production* (Fig. 5b). The majority of genes within these sets has previously been implicated in immune modulatory functions. Strikingly, the EV-high-associated tumors were specifically classified as transcriptional subclass 23 (according to the "Gravendeel" method[23,25]; Fig. 5c). This corresponds to The Cancer Genome Atlas (TCGA) *mesenchymal* subtype.[35] The EV-low-associated tumors were classified as 16/17 or 18 (corresponding to the *neural* or *classical* subtype[35]).

Discussion

GBM patients exhibit severe changes in their immune cell repertoire.[2,3] This is particularly characterized by major alteration of cells of the monocytic lineage, which systemically adapt to a phenotype that is typical for monocytic myeloid-derived suppressor cells.[5,6] In addition, specific types of monocytic cells appear to accumulate in the tumor, where they support tumor growth.[4,7–9] GBM's mechanisms responsible for these alterations
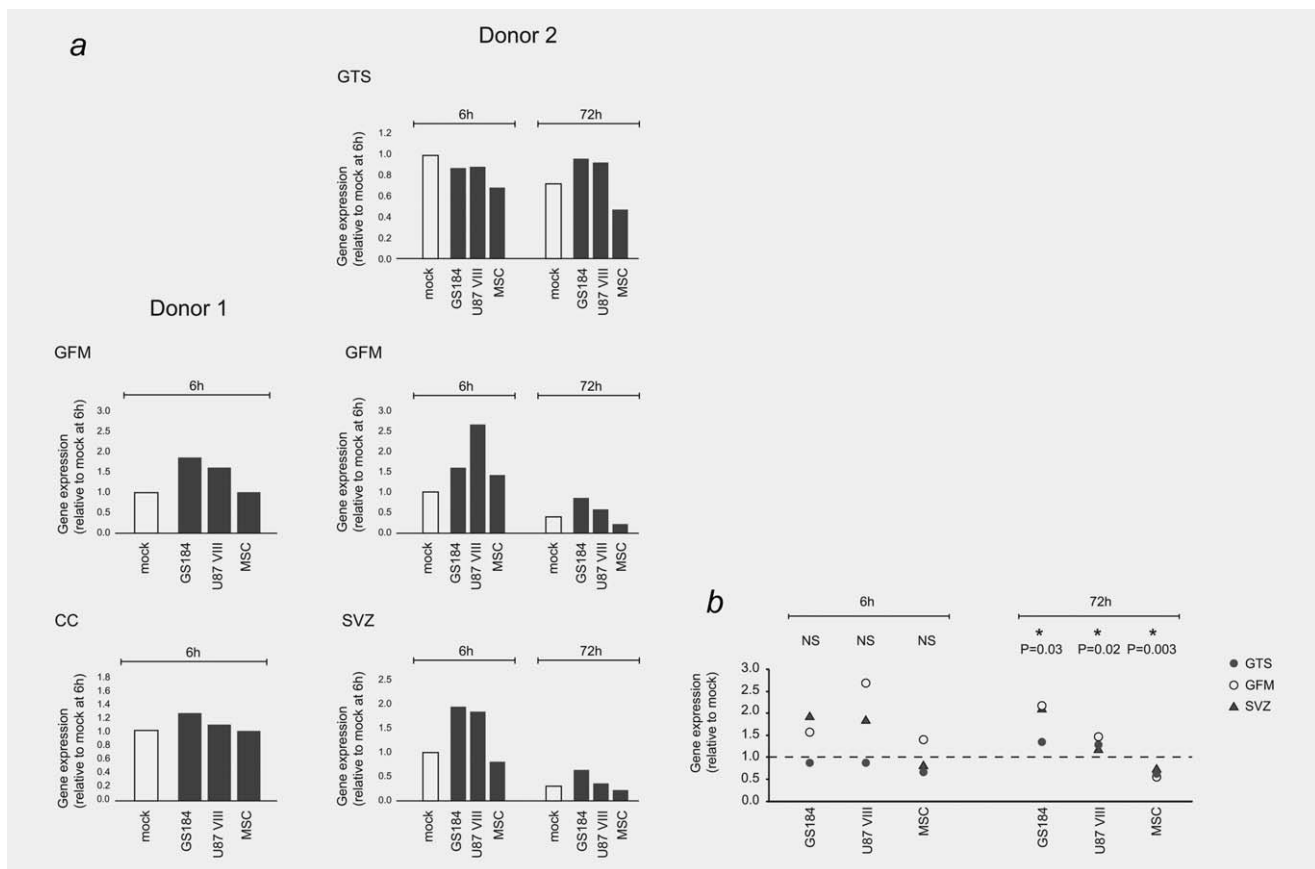
Figure 4. GBM-derived EVs increase MT1-MMP expression in microglia. (*a*) Primary human microglia (isolated from different brain regions of two donors) were incubated for 6 hr or 72 hr with EVs (from GS184, U87-MG/EGFRvIII and MSCs) or mock treated. Q-PCR was used to determine the expression levels of MT1-MMP. At both time points, the expression levels are normalized to the levels obtained after 6 hr mock incubation. (Donor 1 = Parkinson's disease donor, Donor 2 = healthy subject). (*b*) Graph displaying the results of each EV type, with grouping of the GTS, GFM and SVZ data (Donor 2). The 6hr-mock and 72hr-mock incubations were used to normalize the levels obtained for the 6hr-EV and 72hr-EV incubations. The mock values are indicated by the dotted line. Significant differences between EV incubations and mock incubations (determined by two-tailed *t*-test) are indicated by asterisks and *p* values. (GTS = gyrus frontalis medius, GFM = gyrus temporalis superior, CC = corpus callosum, SVZ = subventricular zone).

remain to be elucidated. In this report, we demonstrate that the phenotype of monocytic cells is affected by EVs released by GBM cells.

To better understand the modes of action of GBM-derived EVs, we first performed detailed proteomic profiling. This revealed the selective enrichment in EVs of proteins functioning in *focal adhesion* and *leukocyte transendothelial migration*. Possibly, GBM cells have acquired mechanisms to selectively incorporate these proteins in EVs, thereby facilitating tumor-supporting changes in recipient cells. The findings of our proteomic analyses further strengthened the hypothesis that GBM EVs can modify monocytic cells, including macrophages. Focal adhesion complexes are highly important in the biology of macrophages, to support proliferation, phagocytosis and motility.[8]

Interestingly, multiple proteins were identified in the membrane of GBM EVs that appear to be undetectable in EVs of nontumor origin, as concluded from a large survey in the EVpedia database (http://evpedia.info/; Table 1). These

proteins include lactadherin, syntenin-1, myristoylated alanine-rich C-kinase substrate (MARCKS), integrin alpha-V, integrin alpha-3 and EGFR, which were all detected in both GS184 EVs and U87-MG/EGFRvIII E*v*s. These findings may be of diagnostic value as well. Technologies to detect and quantify EVs in bodily fluids, which would allow for noninvasive diagnostics for GBM, are currently under development.[27,36–39]

GBM patients are in general characterized by aberrations in their T cell compartment, for instance characterized by a general CD4 T cell lymphopenia.[3] Our analyses revealed no signs of EV-induced death of T cells (Supporting Information Fig. S3*c*). This is in contrast to the effects observed for EVs from other types of cancer (*i.e.,* from ovarian, oral and prostate cancer).[40–42]

We observed strong effects of GBM-derived EVs on the phenotype of monocytes. Incubation of PBMCs with U87-MG/EGFRvIII and GS184 EVs resulted in reduced expression of HLA-DR and increased expression of CD14 on the cell surface. Of interest, a similar CD14^high^/HLA-DR^low^
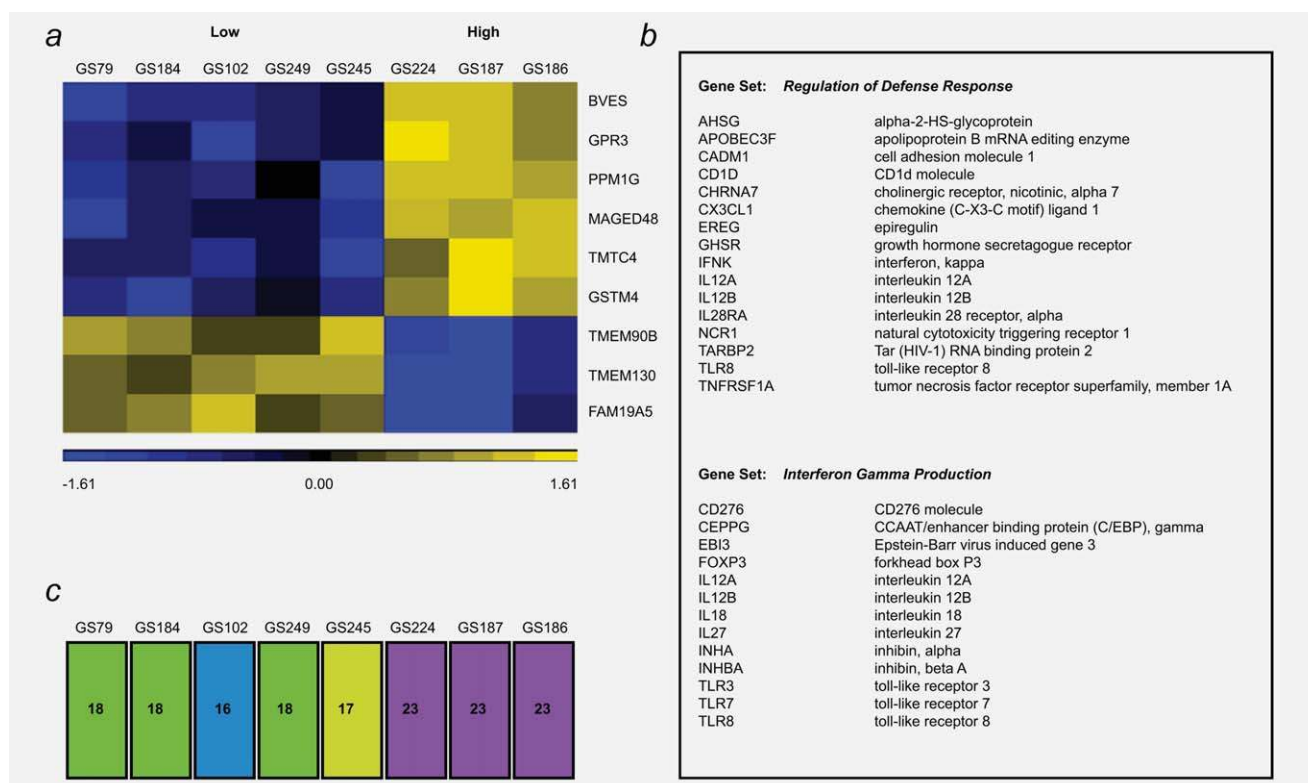
Figure 5. Gene expression analysis of tumors. EV secretion of the GSC cultures was used as a discriminating factor to categorize tumors as *EV-low-associated* or *EV-high-associated* (EV-low: GS79, GS102, GS184, GS245, GS249; EV-high: GS186, GS187, GS224). Expression of genes was determined by microarray analysis.[23] (*a*) Heat map showing differentially expressed genes ($p < 0.01$) in the *EV-high-associated* or *EV-low-associated* group. (*b*) GSEA to identify the most significantly enriched gene sets in the *EV-high-associated* group (False Discovery Rate < 10%, Normalized Enrichment Scores: *Regulation of Defense Response* = 2.01, *Interferon Gamma Production* = 1.97). (*c*) Gene-expression based classification of the tumors.[23,25] Note that classification as either 16/17, 18 or 23 corresponds to a TCGA-based classification as, respectively, *neural*, *classical* or *mesenchymal*.[35] [Color figure can be viewed in the online issue, which is available at wileyonlinelibrary.com.]

phenotype, resembling myeloid-derived suppressor cells, is regularly observed in the systemic monocyte population of GBM patients.[6,31,32] Still, our findings did not point toward EVs in the blood of patients as inducers of this phenotype; isolated EVs (consisting of the total pool of plasma EVs, including GBM and non-GBM EVs) did not change HLA-DR and CD14 on naïve monocytes (Fig. 2*d*). It is likely, however, that the particular experimental procedure was insufficient to faithfully simulate the systemic biodistribution of GBM EVs in patients. Possibly, GBM-derived EVs accumulate at specific locations in the body where they are in contact with monocytes or their precursors. Such a mechanism has been described for melanoma-derived EVs, which home to sites in the bone marrow.[15] Alternatively, monocytes may migrate to the tumor site where they receive high numbers of tumor-derived EVs, followed by redistribution of the cells to the peripheral blood stream.

GBM-derived EVs considerably affected the differentiation of monocytes into macrophages, which was in contrast to EVs derived from cells of non-GBM origin. The phenotypic changes included modified expression of cell surface molecules (*i.e.,* increased CD14, CD16, CD32, CD45, CD163 and

HLA-DR expression) and increased secretion of IL-6, MCP-1 and VEGF, thereby resembling the phenotype of M2-type/ "alternatively activated" macrophages. Presumably, the modified cytokine secretion will severely impact the tumor surroundings. As such, secretion of IL-6 may stimulate GBM proliferation and resistance to therapy.[43] The GBM EVs also induced an increased phagocytic capacity of macrophages (Fig. 3*e*), which may facilitate the migration of tumor cells as a result of enhanced degradation of extracellular matrix components.[44,45]

By implementing a novel technology for EV quantification (tRPS, which allows for particle measurement instead of bulk-protein measurement[27]) we were technically successful in comparing the EV secretion between a panel of different GSC cultures. Surprisingly, this revealed remarkable variation, with some cultures, in particular these from mesenchymal GBM, displaying higher EV secretion levels as compared to others. The mesenchymal EVs were not only characterized by higher secretion levels, but also by more pronounced effects on monocyte to macrophage differentiation. This suggests that EV secretion occurs at higher levels, and may be of higher relevance, in mesenchymal GBMs. Interestingly,

Tumor Immunology

Tumor Immunology

Table 1. Membrane proteins in GS184 EVs

Protein name	Gene name	Detection (Nr of peptides)	Detection (Percentage)	Detected in U87-MG/EGFRvIII EVs
Chondroitin sulfate proteoglycan 4	CSPG4	62	7.0	+
Lactadherin	MFGE8	37	4.2	+
Keratin, type II cytoskeletal 1	KRT1	35	3.9	
Laminin subunit beta-1	LAMB1	34	3.8	
Immunoglobulin superfamily member 8	IGSF8	31	3.5	+
Heat shock cognate 71 kDa protein	HSPA8	29	3.2	+
Syntenin-1	SDCBP	28	3.1	+
Myristoylated alanine-rich C-kinase	MARCKS	23	2.6	+
Moesin	MSN	23	2.6	
Catalase	CAT	22	2.4	
Integrin beta-1	ITGB1	19	2.1	+
Gap junction alpha-1 protein	GJA1	17	1.9	
Sodium/potassium-transporting ATPase	ATP1A1	16	1.8	+
Radixin	RDX	15	1.7	
MARCKS-related protein	MARCKSL1	15	1.7	+
Cofilin-1	CFL1	13	1.4	
Laminin subunit alpha-1	LAMA1	12	1.3	
Neuronal membrane glycoprotein M6-a	GPM6A	11	1.2	
Protocadherin gamma-C3	PCDHGC3	11	1.2	
Ezrin	EZR	11	1.2	
Protocadherin Fat 1	FAT	11	1.2	
Integrin alpha-V	ITGAV	10	1.1	+
Protein tweety homolog 3	TTYH3	10	1.1	
Protein tweety homolog 1	TTYH1	10	1.1	
Integrin alpha-3	ITGA3	9	1.0	+
Serotransferrin	TF	9	1.0	
Neuromodulin	GAP43	9	1.0	
Epidermal growth factor receptor	EGFR	8	0.9	+
CD44 antigen	CD44	8	0.9	+
Glycogen phosphorylase, liver form	PYGL	7	0.7	
2',3'-cyclic-nucleotide 3'-phosphodiesterase	CNP	7	0.7	
4-trimethylaminobutyraldehyde	ALDH9A1	7	0.7	
Neural cell adhesion molecule 1	NCAM1	7	0.7	+
Guanine nucleotide-binding protein G(i), a2	GNAI2	7	0.7	
Basigin	BSG	7	0.7	
AP-2 complex subunit mu-1	AP2M1	7	0.7	
60 kDa heat shock protein, mitochondrial	HSPD1	7	0.7	

The table further includes TUMOR and HEALTHY cell-type columns (Bladder cancer cells, Chronic lymphocytic leukemia B-cells, Colorectal cancer cells, Malignant ascites, Mantle cell lymphoma B-cells, Medulloblastoma cells, Melanoma cells, Osteosarcoma cells, Prostate cancer cells, Small cell lymphoma B-cells, Squamous carcinoma cells; B cells, Breast milk, Carotid atherosclerotic plaque, Endothelial cells, Epididymal fluid, Keratinocytes, Mesenchymal stem cells, Monocytes, Neonatal myoblast cell, Neural stem cells, Platelet, Red blood cells, Retinal pigment epithelium cells, Saliva, Blood/Serum/Plasma, Seminal fluid, Trabecular meshwork cells, Trophoblast cells, T-lymphocytic cell, Umbilical vascular endothelial cells, Urine) with presence indicated by markers.

Proteins were selected with *plasma membrane*-association and sorted on their incorporation level. Proteins are shown with incorporation level exceeding 0.75%. The EVpedia database (http://EVpedia.info/) was used to assess presence of the detected proteins in EVs of other (tumor as well as healthy) origins. Proteins that are not detected in *blood/serum/plasma*, while detected in both GS184 and U87-MG/EGFRvIII EVs are indicated in bold. [Color figure can be viewed in the online issue, which is available at wileyonlinelibrary.com.]

mesenchymal GBMs display an increased infiltration of tumor-supportive monocytic cells, as a result of currently unknown mechanisms.[46,47]

Our findings on macrophages provided a strong rationale to analyze the effects of GBM EVs on brain-resident microglia, which (besides the peripheral-derived macrophages) constitute large part of the monocytic cell population in GBMs' microenvironment. Interestingly, the microglia's response to GBM EVs appeared to differ from the responses observed upon monocyte-to-macrophage differentiation. Expression of cell surface markers HLA-DR and CD163 was not significantly altered (Supporting Information Fig. 6). Despite their overlapping functions,[48] macrophages and microglia are highly different cell types, and it is therefore conceivable that they respond differently to EVs.

We hypothesized that TLR-2, a monocytic receptor, is involved in our observed phenomena. GBM EVs are highly abundant in small RNA molecules,[49] which were previously reported as potent binders to TLRs.[19] TLR-2 binding, followed by down-stream expression of MT1-MMP, has been implicated in the establishment of M2-type characteristics in GBM-associated microglia.[33,34] We did not find evidence for an effect of GBM EVs on MT1-MMP expression in the context of monocyte-to-macrophage differentiation (Supporting Information Fig. S5*b*). However, MT1-MMP was significantly up-regulated by GBM EVs in microglia (Fig. 4). This strongly suggests that EVs are a mechanism for GBMs to induce MT1-MMP expression in GBM-associated microglia, thereby supporting tumor growth. Effects of GBM EVs on monocytic cells of nonmicroglia type (monocytes/macrophages) appear to occur *via* a different mechanism, not involving MT1-MMP.

The therapeutic potential of targeting GBM-associated monocytic cells has already been shown in preclinical models. For example, GBM growth can be inhibited (in proneural GBM models) by blocking colony stimulating factor-1 receptor (CSF-1R), thereby skewing the differentiation of microglia from M2-type to M1-type.[50] Taken together, our findings suggest that similar effects may be obtained by blocking the transfer of GBM EVs to monocytic cells. Indeed, our study identifies for the first time EVs of GBM cells as potent modulators of cells of the monocytic lineage altering them to resemble the tumor-supportive phenotypes described in patients. These findings corroborate on the previously described tumor-supportive effects of GBM-derived EVs on endothelial cells and tumor cells.[16–20] Further research will be imperative to gain more insight into the biology of GBM-derived EVs, which, eventually, may lead to novel (EV-targeted) therapies and/or improvement in current therapies.

References

1. Stupp R, Hegi ME, Mason WP, et al. Effects of radiotherapy with concomitant and adjuvant temozolomide versus radiotherapy alone on survival in glioblastoma in a randomised phase III study: 5-year analysis of the EORTC-NCIC trial. *Lancet Oncol* 2009; 10:459–66.
2. Avril T, Vauleon E, Tanguy-Royer S, et al. Mechanisms of immunomodulation in human glioblastoma. *Immunotherapy* 2011; 3:42–4.
3. Waziri A. Glioblastoma-derived mechanisms of systemic immunosuppression. *Neurosurg Clin N Am* 2010; 21:31–42.
4. da Fonseca AC, Badie B. Microglia and macrophages in malignant gliomas: recent discoveries and implications for promising therapies. *Clin Dev Immunol* 2013; 2013:264124.
5. Kohanbash G, Okada H. Myeloid-derived suppressor cells (MDSCs) in gliomas and glioma-development. *Immunol Invest* 2012; 41: 658–79.
6. Gustafson MP, Lin Y, New KC, et al. Systemic immune suppression in glioblastoma: the interplay between cd14+HLA-DRlo/neg monocytes, tumor factors, and dexamethasone. *Neuro Oncol* 2010; 12:631–44.
7. Gabrusiewicz K, Ellert-Miklaszewska A, Lipko M, et al. Characteristics of the alternative phenotype of microglia/macrophages and its modulation in experimental gliomas. *PLoS One* 2011; 6:e23902
8. Ellert-Miklaszewicz A, Dabrowski M, Lipko M, et al. Molecular definition of the pro-tumorigenic phenotype of glioma-activated microglia. *Glia* 2013; 61:1178–90.
9. Prosniak M, Harshyne LA, Andrews DW, et al. Glioma grade is associated with the accumulation and activity of cells bearing m2 monocyte markers. *Clin Cancer Res* 2013; 19:3776–86.
10. Han SJ, Zygourakis C, Lim M, et al. Immunotherapy for glioma: promises and challenges. *Neurosurg Clin N Am* 2013; 23:357–70.
11. Gyorgy B, Szabo TG, Pasztoi M, et al. Membrane vesicles, current state-of-the-art: emerging role of extracellular vesicles. *Cell Mol Life Sci* 2011; 68: 2667–88.
12. EL Andaloussi S, Mager I, Breakefield XO, et al. Extracellular vesicles: biology and emerging therapeutic opportunities. *Nat Rev Drug Discov* 2013; 12:347–57.
13. Al-Nedawi K, Meehan B, Rak J. Microvesicles: messengers and mediators of tumor progression. *Cell Cycle* 2009; 8:2014 8:
14. Bobrie A, Krumeich S, Reyal F, et al. Rab27a supports exosome-dependent and -independent mechanisms that modify the tumor microenvironment and can promote tumor progression. *Cancer Res* 2012; 72:4920–30.
15. Peinado H, Aleckovic M, Lavotshkin S, et al. Melanoma exosomes educate bone marrow progenitor cells toward a pro-metastatic phenotype through MET. *Nat Med* 2012; 18:883–91.
16. Al-Nedawi K, Meehan B, Micallef J, et al. Intercellular transfer of the oncogenic receptor EGFR-vIII by microvesicles derived from tumour cells. *Nat Cell Biol* 2008; 10:619–24.
17. Al-Nedawi K, Meehan B, Kerbel RS, et al. Endothelial expression of autocrine VEGF upon the uptake of tumor-derived microvesicles containing oncogenic EGFR. *Proc Natl Acad Sci USA* 2009; 106:3794–9.
18. Skog J, Wurdinger T, van Rijn S, et al. Glioblastoma microvesicles transport RNA and proteins that promote tumour growth and provide diagnostic biomarkers. *Nat Cell Biol* 2008; 10:1470–6.
19. Li CC, Eaton SA, Young PE, et al. Glioma microvesicles carry selectively packaged coding and noncoding RNAs which alter gene expression in recipient cells. *RNA Biol* 2013;10.
20. Bronisz A, Wang Y, Nowicki MO, et al. Extracellular vesicles modulate the glioblastoma microenvironment via a tumor suppression signaling network directed by miR-1. *Cancer Res* 2014; 74: 738–50.
21. Post GR, Dawson G. Characterization of a cell line derived from a human oligodendroglioma. *Mol Chem Neuropathol* 1992; 16:303–17.
22. Knaan-Shanzer S, van de Watering MJ, van der Velde I, et al. Endowing human adenovirus serotype 5 vectors with fiber domains of species B greatly enhances gene transfer into human mesenchymal stem cells. *Stem Cells* 2005; 23:1598–607.
23. Balvers RK, Kleijn A, Kloezeman JJ, et al. Serum-free culture success of glial tumors is related to specific molecular profiles and expression of extracellular matrix-associated gene modules. *Neuro Oncol* 2013; 15:1684–95.
24. Fael Al-Mayhani TM, Ball SL, Zhao JW, et al. An efficient method for derivation and propagation of glioblastoma cell lines that conserves the

molecular profile of their original tumours. *J Neurosci Methods* 2009; 176:192–9.

25. Gravendeel LA, Kouwenhoven MC, Gevaert O, et al. Intrinsic gene expression profiles of gliomas are a better predictor of survival than histology. *Cancer Res* 2009; 69:9065–72.

26. Thery C, Amigorena S, Raposo G, et al. Isolation and characterization of exosomes from cell culture supernatants and biological fluids. *Curr Protoc Cell Biol* 2006;Chapter 3:Unit 3 22.

27. de Vrij J, Maas SL, van Nispen M, et al. Quantification of nanosized extracellular membrane vesicles with scanning ion occlusion sensing. *Nanomedicine (Lond)* 2013; 8:1443–58.

28. Maas SL, De Vrij J, Broekman ML. Quantification and size-profiling of extracellular vesicles using tunable resistive pulse sensing. *J Vis Exp* 2014; e51623.

29. Dekker LJ, Zeneyedpour L, Brouwer E, et al. An antibody-based biomarker discovery method by mass spectrometry sequencing of complementarity determining regions. *Anal Bioanal Chem* 2011; 399:1081–91.

30. Franceschini A, Szklarczyk D, Frankild S, et al. STRING v9.1: protein-protein interaction networks, with increased coverage and integration. *Nucleic Acids Res* 2013; 41:d808–15.

31. Woiciechowsky C, Asadullah K, Nestler D, et al. Diminished monocytic HLA-DR expression and ex vivo cytokine secretion capacity in patients with glioblastoma: effect of tumor extirpation. *J Neuroimmunol* 1998; 84:164–71.

32. Ogden AT, Horgan D, Waziri A, et al. Defective receptor expression and dendritic cell differentiation of monocytes in glioblastomas. *Neurosurgery* 2006;59:902–9; discussion 9-10.

33. Markovic DS, Vinnakota K, Chirasani S, et al. Gliomas induce and exploit microglial MT1-

MMP expression for tumor expansion. *Proc Natl Acad Sci U S A* 2009; 106:12530–5.

34. Vinnakota K, Hu F, Ku MC, et al. Toll-like receptor 2 mediates microglia/brain macrophage MT1-MMP expression and glioma expansion. *Neuro Oncol* 2013; 15:1457–68.

35. Verhaak RG, Hoadley KA, Purdom E, et al. Integrated genomic analysis identifies clinically relevant subtypes of glioblastoma characterized by abnormalities in PDGFRA, idh1, EGFR, and nf1. *Cancer Cell* 2010; 17:98–110.

36. Nolte-'t Hoen EN, van der Vlist EJ, Aalberts M, et al. Quantitative and qualitative flow cytometric analysis of nanosized cell-derived membrane vesicles. *Nanomedicine* 2011; 8:712–20.

37. Shao H, Chung J, Balaj L, et al. Protein typing of circulating microvesicles allows real-time monitoring of glioblastoma therapy. *Nat Med* 2012; 18:1835–40.

38. Dragovic RA, Gardiner C, Brooks AS, et al. Sizing and phenotyping of cellular vesicles using nanoparticle tracking analysis. *Nanomedicine* 2011; 7:780–8.

39. Maas SL, de Vrij J, van der Vlist EJ, et al. Possibilities and limitations of current technologies for quantification of biological extracellular vesicles and synthetic mimics. *J Control Release* 2015; 200:87–96.

40. Taylor DD, Gercel-Taylor C, Lyons KS, et al. Tcell apoptosis and suppression of T-cell receptor/CD3-zeta by fas ligand-containing membrane vesicles shed from ovarian tumors. *Clin Cancer Res* 2003; 9:5113 9:

41. Kim JW, Wieckowski E, Taylor DD, et al. Fas ligand-positive membranous vesicles isolated from sera of patients with oral cancer induce apoptosis of activated T lymphocytes. *Clin Cancer Res* 2005; 11:1010–20.

42. Abusamra AJ, Zhong Z, Zheng X, et al. Tumor exosomes expressing fas ligand mediate cd8+ T-cell apoptosis. *Blood Cells Mol Dis* 2005; 35: 169–73.

43. Sasaki A, Ishiuchi S, Kanda T, et al. Analysis of interleukin-6 gene expression in primary human gliomas, glioblastoma xenografts, and glioblastoma cell lines. *Brain Tumor Pathol* 2001; 18:13–21.

44. Rey-Giraud F, Hafner M, Ries CH. In vitro generation of monocyte-derived macrophages under serum-free conditions improves their tumor promoting functions. *PLoS One* 2012; 7: e42656

45. Wels J, Kaplan RN, Rafii S, et al. Migratory neighbors and distant invaders: tumor-associated niche cells. *Genes Dev* 2008; 22:559–74.

46. Rutledge WC, Kong J, Gao J, et al. Tumor-infiltrating lymphocytes in glioblastoma are associated with specific genomic alterations and related to transcriptional class. *Clin Cancer Res* 2013; 19: 4951–60.

47. Engler JR, Robinson AE, Smirnov I, et al. Increased microglia/macrophage gene expression in a subset of adult and pediatric astrocytomas. *PLoS One* 2012; 7:e43339

48. Butovsky O, Jedrychowski MP, Moore CS, et al. Identification of a unique TGF-beta-dependent molecular and functional signature in microglia. *Nat Neurosci* 2014; 17:131–43.

49. Fabbri M, Paone A, Calore F, et al. MicroRNAs bind to Toll-like receptors to induce prometastatic inflammatory response. *Proc Natl Acad Sci U S A* 2012; 109:E2110–6.

50. Pyonteck SM, Akkari L, Schuhmacher AJ, et al. CSF-1R inhibition alters macrophage polarization and blocks glioma progression. *Nat Med* 2013; 19:1264–72.

Tumor Immunology